Key Engineering Materials
ISSN: 1662-9795, Vol. 1047, pp 65-71

Submitted: 2025-12-18
Revised: 2026-02-18
Accepted: 2026-02-25
Online: 2026-04-13

Evaluation of SLA Biocompatible Resins Properties for Use as Dielectric Layers in 3D Printed Capacitive Force Sensors

Alessandro Epicoco[1,a], Tiziano Fapanni[2,b], Stefano Pandini[1,c], Paola Serena Ginestra[1,d], Elisabetta Ceretti[1,e], Emilio Sardini[2,f], Miriam Seiti[1,g*]

[1]Department of Mechanical and Industrial Engineering, University of Brescia, IT

[2]Department of Information Engineering, University of Brescia, IT

[a]a.epicoco001@unibs.it, [b]tiziano.fapanni@unibs.it, [c]stefano.pandini@unibs.it, [d]paola.ginestra@unibs.it, [e]elisabetta.ceretti@unibs.it, [f]emilio.sardini@unibs.it, [g*]miriam.seiti@unibs.it

Keywords: 3D printed capacitive force sensor, SLA, flexible resin, electromechanical properties.

Abstract. Additive manufacturing (AM) technologies have enabled the fabrication of customizable, low-cost capacitive sensors for a wide range of applications, including robotics, automation, and bioelectronics. Although various AM techniques have been explored, structural inconsistencies often remain a challenge, limiting the performance and reproducibility of printed dielectric layers. Stereolithography (SLA), offers higher resolution and denser prints, yet the use of commercial photopolymer resins as dielectric materials remains underexplored. This study investigates two commercial SLA-compatible resins, a flexible medical-grade elastic resin and a dental-grade resin, as potential dielectric layers for capacitive force sensors. Both resins are biocompatible for short-term use or skin contact, making them suitable also for medical applications. The BioMed elastic 50A-V1 resin exhibited a Young's modulus of E = 5.0 ± 0.2 MPa up to approximately 60% strain, whereas the Dental Clear V2 resin showed a significantly higher modulus of E = 1020 ± 80 MPa under the same conditions. Therefore, the elastic resin was subsequently chosen as the dielectric material to fabricate a proof-of-concept capacitive force sensor, which exhibited a final capacitance of 1.13 ± 0.03 pF within a force range of 10 to 400 N. The findings serve as a preliminary step towards the development of fully 3D-printed capacitive force sensors for integration into soft robotic and smart biomedical systems.

Introduction

The rapid advancement of additive manufacturing (AM) technologies has revolutionized the fabrication of electronic components, with 3D printed sensors emerging as a promising area of research. [1] These sensors can be implemented in different fields, such as robotics and clinical practice. [2-3] Recent developments in AM have indeed enabled the fabrication of low cost and easy processable capacitors, with customizable geometries and properties, offering advantages in miniaturization and integration with printed circuit boards. [4-8] In this frame, looking towards the integration of intelligence on everyday objects, [9] AM-based capacitors can be exploited to develop different type of sensors to fabricate smart objects. In a capacitor, the dielectric layer is a critical component determining sensor performance. In fact, the properties of a capacitor depends on its geometric properties and the type of dielectric used. [10] However, dielectric materials for capacitive sensing applications can vary widely and include substances like ceramics, thermoplastics, metal oxides, or even air. [11-12] In order to explore the capabilities offered by AM technologies, different works in the literature focus on various techniques, such as Fused Deposition Modelling (FDM) and stereolithography (SLA). [13-17] Although promising results, the performance of these techniques in producing dielectric printed layers remains a critical limitation, especially in processes like FDM, which inherently introduces structural inhomogeneities due to incomplete inter-line and inter-layer fusion. [12] This variability compromises the reliability and reproducibility of FDM-printed capacitors. On the other hand, Vat Photopolymerization (VPP) and in particular masked SLA, usually offers higher resolution and denser part structures than FDM, [18] leading to more consistent results.

However, while FDM materials have been explored as dielectric components, there remains a significant gap in the literature regarding the use of commercial SLA photopolymerizable resins. [19-22] Therefore, this study evaluates the mechanical properties of two commercial SLA resins, a flexible medical-grade elastic resin and a dental-grade resin, for use as dielectric layers in SLA-printed capacitive sensors. Being biocompatible for short-term use or skin contact, these resins can also be applied in medical applications. A proof-of-concept capacitive force sensor is fabricated using the best performing resin to evaluate the feasibility of the material as dieletric. The results presented provide a preliminary investigation towards the development and fabrication of fully 3D-printed capacitive force sensors for soft robotics.

Materials and Methods

Materials

Two photocurable epoxy resins were chosen as the main dielectric layer materials: i) BioMed Elastic 50A-V1 and ii) Dental Clear V2 (Formlabs, USA). BioMed Elastic 50A-V1 is designed for soft tissue models and has a biocompatibility compliant with ISO 13485 standards, ensuring safety for long-term skin contact and short-term contact with mucous membranes. Dental Clear V2 (ISO 10993) dental exhibit reduced elasticity compared to 50A-V1, but has significantly superior mechanical properties, making it a prevalent choice for the fabrication of resilient occlusal splints. Table 1 shows the mechanical properties of the BioMed Elastic 50A-V1 and Dental Clear V2 resins. Copper (Cu) tape was selected as conductive electrode material. Isopropanol (IPA, Sigma Aldrich, IT) and distilled water (DI) were used as cleaning solvents.

Manufacturing process

A Prusa© SL1 Speed (CZ) SLA bottom-up system was used to produce the samples. SLA uses a high-resolution LCD screen to project a mask of the intended layer onto a vat of liquid resin, where an ultra-violet (UV) light source solidifies the resin. The energy provided by the laser activates photo initiators present in the resin, initiating a chemical reaction that induces the polymerization of the monomers. Samples with different heights and three replicas for each resin were printed. Process parameters are reported in Table 2. Post-printing processes were performed using a Prusa Washing and Curing Machine for 10 and 15 minutes, respectively (CW1, Prusa©, CZ).

Materials Characterization

Mechanical tests were performed using a dynamometer (Instron 3366, DE). The samples were mechanically tested by applying a force from 0 to 9000N. Samples dimensions were 7 x 7 mm, with a variable thickness equal to 4.00 and 5.00 mm for both resins.

Table 1. Properties of selected SLA materials.

Property	BioMed Elastic 50A-V1	Dental LT Clear V2
Density (g/cm³)	1.1	1.09
Elastic Modulus (GPa)	0.0016–0.0032	2.08
Poisson's Ratio	0.3	0.35
Constitutive Model	Hyperelastic	Linear elastic

Table 2. SLA process parameters selected.

Process parameter	BioMed Elastic 50A-V1 & Dental LT Clear V2
Time 1st layer	50 s
Time 2nd layer	30 s
Thickness layer	0.03 mm
Height (z)	4.00, 5.00 mm
Dimensions (x,y)	7.00 x 7.00 mm

The crosshead speeds were adopted to have a strain rate equal to 1 min^{-1}. Three replicas were tested for each condition analysed.

Device Electrical Characterization

To characterize the suitability of the selected material as force sensors, three 7 x 7 x 2 mm samples were prepared with conductive Cu tape to produce a set of capacitive devices. The experimental setup consists of an Instron test system (Model 3366), equipped with a 10 kN load cell. The uniaxial compression tests were performed at room temperature by using two planar compression platens with a 8 cm diameter to apply 10 load-unload cycles between two load targets of 10 and 400 N. Subsequently, 5 additional cycles with alternating maximum load peaks of 170 N and 270 N were carried out to assess the repeatability of the measurements after an appropriate preload phase.
Kapton foils were used as insulators during measurement acquisition process. The crosshead speed was specifically chosen to have a strain rate approximately equal to 1 min^{-1}. For each test, the load vs crosshead displacement curve and the electrical capacitance signals were recorded over time. To measure the relevant electrical components, an MFIA 500kHz Impedance Analyzer (Zurich Instruments) was interfaced with a laptop via a custom MATLAB script. The device was configured to sample its impedance at 10 kHz and to continuously monitor and output the corresponding capacitance over time.

Results and Discussion

Process and Material Characterization

Resin-based samples were successfully 3D SLA printed using the same set of print parameters. As illustrated in Fig. 1A, the resin 50A-V1 exhibits a non linear stress increase, with an initial elastic modulus equal to E = 5.0 ± 0.2 MPa, up to about 60% strain (about 8 MPa), followed by a steeper increase afterwards, due to strain hardening and the increase of transverse section.

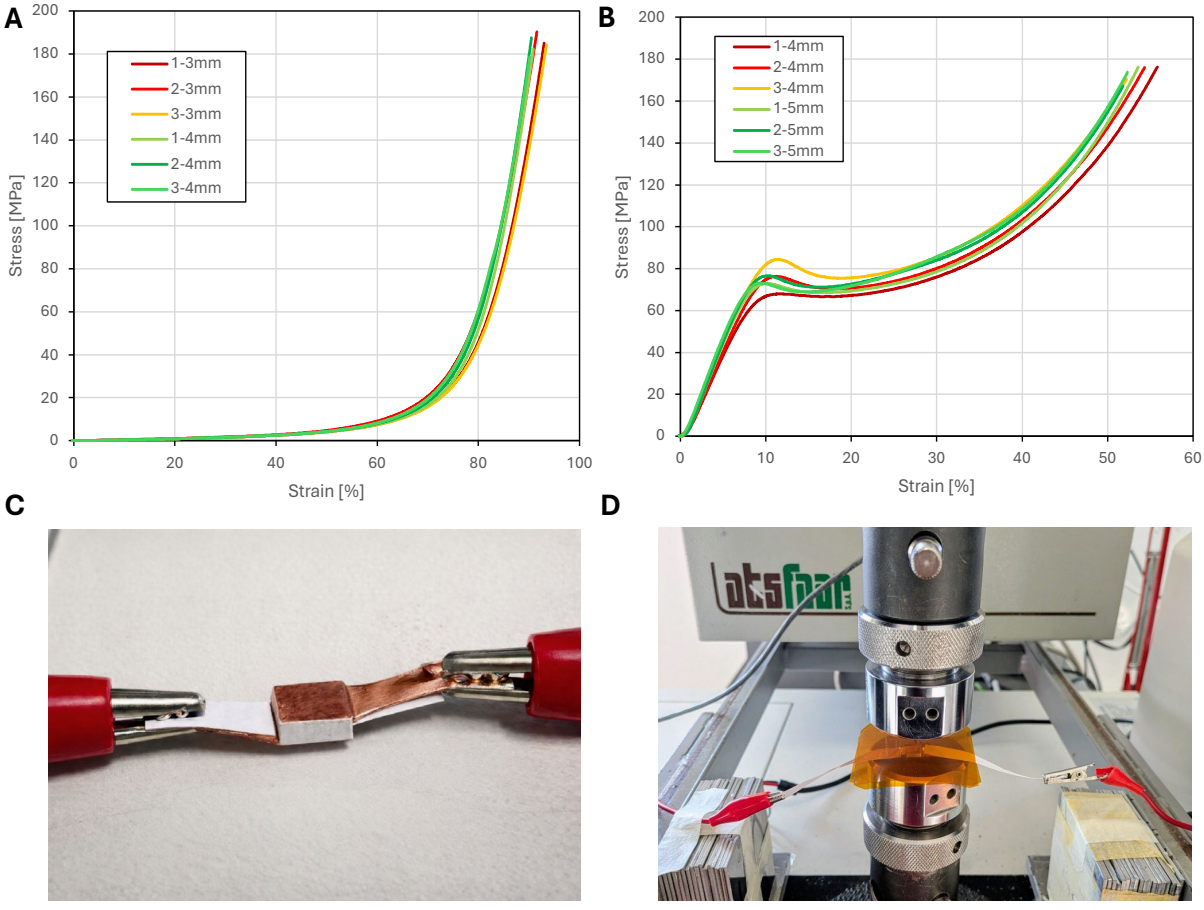

Fig. 1. Mechanical characterization results for the 3D SLA printed (a) 50A-V1 resin and the (b) Dental Clear V2 resin; (c) proof-of-concept force sensor, (d) electromechanical setup.

Contrarily, the Dental Clear V2 resin showed a significantly stiffer behaviour, with an elastic modulus of E = 1020 ± 80 MPa under the same conditions (Fig. 1B), followed by yielding at a stress equal to 75 ± 5 MPa, a subsequent strain softening and a final increase in strain hardening regime. Due to its lower stiffness, 50A-V1 was selected as the dielectric material for the capacitive force sensor, being significantly softer than the Dental Clear V2 resin. Its greater deformability indeed enables larger variations in electrode separation under applied force, which enhances the sensitivity of the sensor. Fig. 1C shows the proof-of-concept force sensor fabricated using the elastic resin 50A-V1.

Electrical Characterization Result

Fig. 1D reports the electromechanical setup used in this study. Fig. 2A shows the force–displacement response of a representative sample, while Table 3 reports the stiffness values obtained by comparing the 1st and the 10th preload cycle for each sample. For all samples, a systematic increase in stiffness (Fig. 2B) is observed between the 1st and the 10th cycle, indicating a progressive mechanical stabilization of the polymeric dielectric under cyclic loading. The percentage variations associated with the two cycles and compared to the average value across all 10 cycles, remain limited, confirming the good repeatability of the mechanical response and the convergence of stiffness values after the initial cycles. Table 4 summarizes the main electromechanical parameters of the sensors.

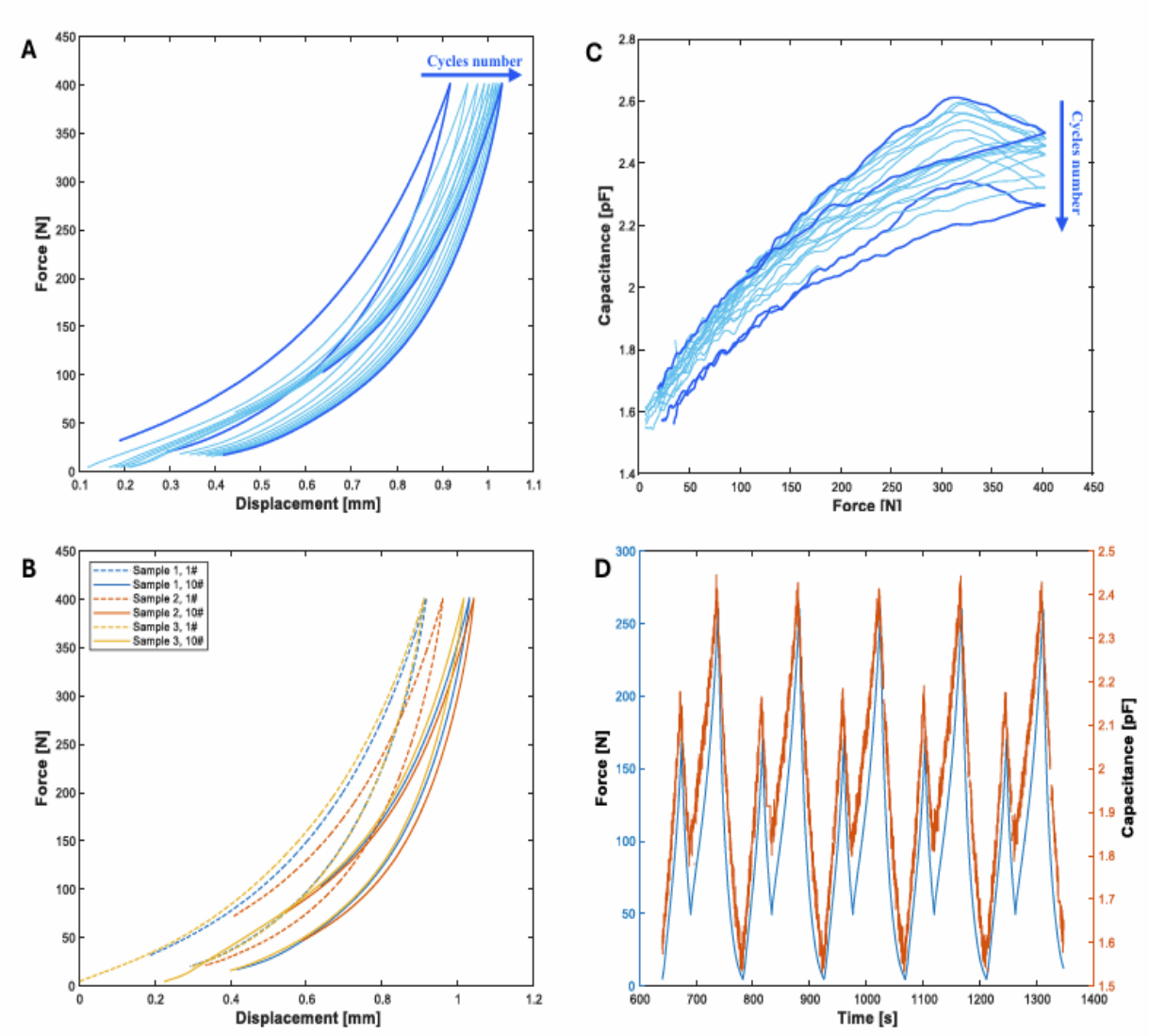

Fig. 2. Electromechanical results for 3D SLA printed samples: a) preload force vs displacement (Sample N°1), b) preload capacitance vs force (Sample N°1), c) force vs displacement of 1st and 10th cycle, d) force and capacitance vs time in controlled cycles after preload.

Table 3. Stiffness values for increasing preload cycle numbers for SLA 3D printed samples.

Sample N°	Stiffness [N/mm]		Δ%	
	1° cycle	10° cycle	1° cycle	10° cycle
1	894.81	1059.83	1.37	0.87
2	908.65	1053.70	2.94	1.45
3	844.57	1093.98	4.32	2.32

Table 4. Main electromechanical parameters of SLA 3D printed samples.

Sample N°	F-D Hysteresis [%]	C-F Hysteresis [%]	Sensitivity [fF/N]	R^2		
1	14.5	12.8	3.08 ± 0.1	0.93		
2	12.1	10.7	3.18 ± 0.1	0.92		
3	12.0	20.7	2.69 ± 0.2	0.93		
Sample N°	C_{MAX}_1°	C_{MAX}_10°	ΔC [pF]	C_{MAX}_11°	C_{MAX}_15°	ΔC [pF]
1	2.26	2.50	0.23	2.37	2.40	0.03
2	2.43	2.58	0.15	2.45	2.47	0.02
3	2.20	2.43	0.23	2.28	2.32	0.04

The observed hysteresis values are consistent with the viscoelastic behavior of the polymeric material and are reflected in the electrical response of the sensors. Despite the presence of hysteretic effects, all sensors exhibit an average sensitivity in the order of 3.0 fF/N and good linearity ($R^2 > 0.9$), confirming that, once mechanically stabilized through the preload cycles, the system provides a reliable and repeatable electromechanical response within the investigated load range. The sensors show a final average capacitance variation of C = 1.13 ± 0.03 pF.

Figure 2C shows the capacitance–force response of a representative sensor during the 10 preload cycles, highlighting the difference between the 1st and 10th cycle. Table 4 also display the maximum capacitance value measured during the 1st and 10th preload cycle, as well as the maximum values recorded during the subsequent five control cycles, together with the corresponding capacitance variation ΔC for each sample. For all samples, an increase in the maximum capacitance (C_{MAX}) is observed, with values ranging approximately between 0.20 and 0.25 pF. This increase is attributed to residual deformation of the polymeric dielectric induced by cyclic loading, which leads to a permanent reduction in the electrode separation and, consequently, to a shift in the absolute capacitance baseline. In contrast, the capacitance variation during the five subsequent cycles is much smaller. Therefore, these results demonstrate that, although the preload induces a baseline shift in the absolute capacitance, the useful capacitive response of the sensor is preserved and it is stable.

Conclusions and future perspectives

This study demonstrates that SLA-compatible photocurable elastic resins can be effectively employed as dielectric layers in capacitive force sensors. In particular, the commercial BioMed Elastic 50A-V1 resin exhibited a stable and repeatable electromechanical behavior, providing an average capacitance variation of 1.13 ± 0.03 pF over a load range of 10–400 N, with an average sensitivity on the order of 3.0 fF/N and good linearity ($R^2 > 0.9$). These results confirm that commercially available elastic resins can act as functional dielectrics for 3D-printed capacitive sensors, without the need for custom materials. The results further show that after 10 load–unload cycles the system reaches a mechanically and electromechanically stable condition, characterized by converging stiffness values, repeatable capacitive response, and limited hysteresis. Although the preload cycles induce a shift in the absolute capacitance value, with an increase in the maximum capacitance on the order of 0.20–0.25 pF, the capacitance variation associated with the applied load (ΔC) remains essentially unchanged, ensuring reliable sensor operation in subsequent measurement phases. Overall, these findings confirm that elastic SLA resins can be used as reliable dielectrics for capacitive force sensors and that a preload phase limited to 10 cycles represents a sufficient mechanical conditioning step to achieve a stable and reproducible response. Future developments will focus on evaluating electromechanical stability under long-term cyclic loading, optimizing the readout electronics, and extending the approach to multi-sensor configurations, with the goal of realizing fully 3D-printed capacitive sensing systems for applications in soft robotics, biomedical devices, and intelligent monitoring systems.

Acknowledgment

The authors acknowledge MICS (Made in Italy – Circular and Sustainable) Extended Partnership (Next Generation EU (Italian PNRR – M4 C2, 1.3–D.D.1551.11–10–2022, PE00000004 CUP D73C22001250001).

References

[1] T. Fapanni, R. Palucci Rosa, E. Cantù, F. Agazzi, N. F. Lopomo, et al., "Overall additive manufacturing of capacitive sensors integrated into textiles: A preliminary analysis on contact pressure estimation," in Proc. Int. Joint Conf. Biomed. Eng. Syst. Technol., 2024, pp. 195–200.

[2] G. Santona, T. Fapanni, A. Fiorentino, F. Doglietto, M. Serpelloni, "Preliminary Study on a 3D Printed Sensorized Probe to Characterize Pituitary Adenoma Hardness", IEEE International Workshop on Metrology for Industry 4.0 & IoT, 2023, pp. 249-253.

[3] J. Yu, P. B. Perera, R. V. Perera, M. M. Valashani, A. Withana, "Fabricating Customizable 3-D Printed Pressure Sensors by Tuning Infill Characteristics," IEEE Sens. J., 2024, vol. 24, no. 6, pp. 7604–7613.

[4] M.S. Hassan, S. Zaman, J.Z.R. Dantzler, D. Hazel Leyva, M.S. Mahmud, J. Montes Ramirez, et al., "3D printed integrated sensors: From fabrication to applications—A review," Nanomaterials, 2023, vol. 13, no. 24, Art. no. 24.

[5] S.H. Kim, U. Jeong, K.J. Cho, "Multiparameter Remote Contact Force Sensor With Embedded Bend Sensing for Tendon-Driven Hand Robots," IEEE ASME Trans. Mechatron., 2024, vol. 29, no. 1, pp. 557–566.

[6] T. Dong, J. Wang, Y. Chen, L. Liu, H. You, T. Li, "Research Progress on Flexible 3-D Force Sensors: A Review," IEEE Sens. J., 2024, vol. 24, no. 10, pp. 15706–15726.

[7] X. Li, Z. Ye, M. Yang, M. Liu, X. Zhang, "Wireless, Fully soft, Pressure and Temperature Sensors for Sensitive and Robust Diabetic Foot Ulcer Monitoring," IEEE SENSORS, 2024, pp. 1–4.

[8] L. Wang, J. Cao, M. Liu, Y. Lv, "Chinese Paper-cutting Inspired Topological Flexible Piezoresistive Pressure Sensor for Wearable Health Monitoring", IEEE SENSORS, 2024, pp. 1–4.

[9] D. Bianchini, T. Fapanni, M. Garda, F. Leotta, M. Mecella, A. Rula, "Digital Thread for Smart Products: A Survey on Technologies, Challenges, and Opportunities in Service-Oriented Supply Chains", IEEE Access, 2024, vol. 12, pp. 125284-125305.

[10] C. Wang, X. Li, H. Jia, S. Liu, X. Liu, T. Minari, et al., "Polymer-based dielectrics with high permittivity and low dielectric loss for flexible electronics," J. Mater. Chem. C, 2022, vol. 10, no. 16, pp. 6196–6221.

[11] A. Giuri, R. Striani, S. Carallo, S. Colella, A. Rizzo, C. Mele, et al., "Waste carbon ashes/PEDOT:PSS nano-inks for printing of supercapacitors," Electrochim. Acta, 2023, vol. 441, p. 141780.

[12] P. Veselý, T. Tichý, O. Šefl, and E. Horynová, "Evaluation of dielectric properties of 3D printed objects based on printing resolution," IOP Conf. Ser. Mater. Sci. Eng., 2018, vol. 461, no. 1, p. 012091.

[13] S. Peng, H. Hassan, S. Rosseel, G.A. Matricali, K. Deschamps, V. Vandeginste, et al., "Recent Advances in 3-D Printed, Wearable Pressure Sensors for Plantar Pressure Monitoring: A Review," IEEE Sens. J., 2024, vol. 24, no. 21, pp. 33903–33921.

[14] R. Bhaumik, T. Preindl, A. Ion, C. Ayala-Garcia, N. Cohen, M .Haller, “Inductive Pressure Sensors Using 3D-Printed Structures With Tunable Stiffness,” IEEE Sens. Lett., 2025, vol. 9, no. 5, pp. 1–4.

[15] X. Guo, H. Li, W. Hong, Y. Zhao, Q. Hong, Y. Xu, “3-D Printed Fourth-Order Star-Like Negative Poisson’s Ratio Structure for High-Sensitivity Bionic Flexible Capacitive Pressure Sensor,” IEEE Sens. J., 2024, vol. 24, no. 9, pp. 13937–13945.

[16] J. Yu, P. B. Perera, R. V. Perera, M. M. Valashani, A. Withana, “Fabricating Customizable 3-D Printed Pressure Sensors by Tuning Infill Characteristics,” IEEE Sens. J., 2024, vol. 24, no. 6, pp. 7604–7613.

[17] M. Seiti, O. Degryse, R. M. Ferraro, S. Giliani, V. Bloemen, E. Ferraris, “3D Aerosol Jet® printing for microstructuring: Advantages and Limitations,” Int. J. Bioprinting, 2023, vol. 9, no. 6, pp. 57–74.

[18] T. Fapanni, J. Agnelli, R. Rosa, G. Rosace, F. Baldi, N. F. Lopomo, et al., “Analysis of polymers for additive manufacturing: Based contact pressure and force sensors,” in Proc. Int. Joint Conf. Biomed. Eng. Syst. Technol., 2025, pp. 180–187.

[19] L. Zhong, J. Du, Y. Xi, F. Wang, L. Wu, J. Li, et al., “Multi-material and parameter-controllable stereolithography 3D printing of graded permittivity composites for high voltage insulators,” Int. J. Smart Nano Mater., 2023, vol. 14, no. 1, pp. 1–16.

[20] Z. Hu, Y. Wang, X. Liu, Q. Wang, X. Cui, S. Jin, “Rational design of POSS containing low dielectric resin for SLA printing electronic circuit plate composites,” Compos. Sci. Technol., 2022, vol. 223, p. 109403.

[21] Y. Yang, Z. Chen, X. Song, B. Zhu, T. Hsiai, P. Wu, et al., “Three dimensional printing of high dielectric capacitor using projection based stereolithography method,” Nano Energy, 2016, vol. 22, pp. 414–421.

[22] M. Seiti, P.S. Ginestra, A. Verma, E. Ceretti, and E. Ferraris, “Aerosol Jet® printing on stereolithography resin substrates for in-vitro dual bioreactor sensing,” Procedia CIRP, 2022, vol. 110, pp. 174–179.